Cement & Concrete Composites 37 (2013) 249–258

Contents lists available at SciVerse ScienceDirect

Cement & Concrete Composites

journal homepage: www.elsevier.com/locate/cemconcomp

Compressive strength of cement-based composites: Roles of aggregate diameter and water saturation degree

M. Szczesniak, T. Rougelot *, N. Burlion, J.-F. Shao

Laboratoire de Mécanique de Lille, UMR CNRS 8107, Université Lille 1, Polytech'Lille, Av. Paul Langevein, 59650 Villeneuve d'Ascq, France

ARTICLE INFO

Article history:
Received 6 January 2011
Received in revised form 2 July 2012
Accepted 3 August 2012
Available online 11 August 2012

Keywords:
Water saturation
Glass beads
Strength
Drying
Triaxial compression
Microtomography
Cracking

ABSTRACT

Concrete structures experience microcracking leading to mechanical damage when submitted to desiccation. This change in mechanical properties can be dependant on the level of drying and also on constituents of the material. This paper focuses on one particular aspect, which is to determine the role of the size of rigid inclusions over cementitious materials under drying. However, concrete is a complex heterogeneous material, where the shape of natural aggregates is variable, and the number of factors to analyze is large. Thus the study was performed on a geometrically simplified material, initially proposed by Bisschop and van Mier (2002) [1] compound of spherical glass inclusions of several diameters in a cementitious matrix to explore the influence of aggregate size. A set of uniaxial and triaxial compressive tests is performed for materials with various water saturation levels. A great dependence is observed between mechanical properties, notably peak strength and damage, linked to aggregate size and water saturation degree. Complementary microtomographic acquisitions are also done, and tend to validate the cracking pattern dependency to the aggregate diameter, and therefore explain changes in mechanical behaviour.

1. Introduction

To understand the mechanical behaviour of concrete under hydric solicitations is a major aspect when studying the durability of such a material [2,3]. Indeed, drying and wetting of concrete, which is a common loading pattern experienced by most of concrete structures during their life, lead to change in the mechanical response of the material [4]. Generally an increase in uniaxial compressive strength with drying is observed [5]. Research over coupling between shrinkage and mechanical behaviour of cementitious based materials has been extensive, either in an experimental way [6,7] or in numerical modelling [8,9]. One particular interesting aspect relies on the influence of drying conditions and saturation level inside concrete over peak strength, modified by development of a crack network. Indeed, due to low permeability and diffusion of such a material, differential shrinkage and expansion between core and exterior part of the structure can be experienced [10,11].

In addition to this macroscopic phenomenon linked to hydric gradients, a more specific study can be performed on a mesoscale. At such a scale, concrete is no more homogenous and should be considered as formed by aggregates included in a cementitious matrix. Each of these constituents has its own physico-chemical and mechanical characteristics. As a result, the observed macroscopic behaviour will be highly linked to a contribution of each constituent properties, that in addition are coupled. For instance, if a closer look is taken on drying of concrete, shrinkage of aggregates (usual siliceous or calcareous sand or gravels are far more rigid than cement paste and considered as "rigid" inclusions later and their dimensions are almost not water-dependent) with decreasing water saturation is generally with some order of magnitude lower than for cementitious matrices. A differential local shrinkage of matrix around a rigid inclusion (due to a difference between Young's modulus of the matrix and aggregates) may lead to orthoradial tensile stresses and, due to low tensile strength of the cementitious matrix, a potential way of crack nucleation [12,13]. This phenomenon is called "aggregate restraining effect". As a consequence, the damage and the global cracking pattern, including micro and macro-cracks, will be dependent of this local effect, in addition to the structural one.

A refined analysis of the local role of aggregates should be developed in the framework of micromechanics. Recent numerical and theoretical techniques have been proposed to model such complex cementitious materials. The increase in computational capabilities and the development of numerical procedures allow modelling these heterogeneous materials at a lower scale. For example, some authors are interested in micromechanics [14] to describe the behaviour of frictional geomaterials such as concrete [15]. The framework of microporomechanics [16] is suitable in hydro-mechanical modelling which takes into account the microscopic scale. They aim at modelling the behaviour of inclusions surrounded

* Corresponding author.
E-mail address: thomas.rougelot@polytech-lille.fr (T. Rougelot).

0958-9465/$ - see front matter © 2012 Elsevier Ltd. All rights reserved.
http://dx.doi.org/10.1016/j.cemconcomp.2012.08.001

by a matrix, and then by a repetition of this phase arrangement, to get the macroscopic behaviour or characteristics of such a material. However, this kind of approach is still under development, in particular in aiming at reliably modelling the link between strength for different water saturation. Experimental investigations are thus necessary, in order to validate the proposed models or to highlight the physical phenomena and properties to take into account.

Linked to this local effect, a focus on the size diameter of aggregates is of a notable interest. Concretes are composed of several types of aggregates, whose main characterisation, at least in a first step, is a granulometric curve. Knowing how each size of aggregates will contribute to the macroscopic behaviour has practical meaning. On this basis, some conclusions could be drawn on the future material durability and performance, without a detailed experimental campaign each time the granulometric curve is modified. Moreover, during the setting of concrete inside a mould, segregation may appear and leads to inhomogeneous repartition of aggregates [17]. In addition, due to wall-effect, small particles will be in a greater proportion close to surface of the concrete element [18]. A different mechanical behaviour due to these effects might occur, notably impacted by a change in the cracking pattern or damage state, and will modify the strength. In the same way, the porosity and transport properties may be modified, and have to be dealt with for a reliable estimation of durability.

Finally, a last aspect has to be investigated as regards inclusions in a matrix: the interfacial behaviour. This area (called ITZ, Interfacial Transition Zone) is mainly due to wall-effect leading to an increase of water-to-cement ratio around inclusions [19]. It has generally reduced mechanical and physico-chemical performances, with a higher porosity [20] and a lower Young's modulus for instance [21], at least near (about 20 to 50 μm), around each aggregate [19,20]. The global behaviour of the concrete could therefore be influenced by the properties of this interface. One noticeable point is that the total surface of contact zone between inclusions and cementitious matrix depends on the shape of aggregates and in particular of their diameter. For a spherical particle, its specific surface is inversely proportional to the squared-diameter of inclusions. As a result, the effect of this interface could be important for small particles, as it represents an increasing proportion of the material. However, some recent results tend to show that this effect may remain quite low on the global behaviour of concrete, notably under uniaxial compression [22] or for diffusivity [23]. A negative influence of this interface on compressive strength has been detected under leaching [24]. However, the leaching conducts to a chemical modification of the microstructure, in particular in the ITZ, which is rich in Portlandite. Comparing this evolution of microstructure with the one expected from desaturation remains hard. In a second time, for a given volume proportion of aggregates inside a concrete, an increase in the specific surface implies an increase in number of rigid inclusions that can behave as crack nucleation point. The cracking pattern should therefore be more widespread (i.e. a smaller inter-distance between two cracks in a composite with small inclusions) inside the cementitious matrix, and may influence the global strength of the material. Nevertheless, if hydric gradients during drying exist through the concrete specimen, the cracking pattern might appear firstly only in the outer part (in contact with environment) and progressively develop inside the core as shown in [25].

Concerning the effect of inclusion diameter, Some experiments have recently shown on several nanocomposites that adding nano-inclusions inside a matrix may lead to a drastic improvement of the mechanical characteristics of a material [26]. Additional work on polymeric composites with small volumetric fraction of glass beads validates this tendency where tensile strength is higher for 6 μm inclusions than for 500 μm [27]. About concrete, the effect of aggregate distribution on compressive strength is somehow more complex, as aggregate is a complex component with many varying properties (size, roughness, shape, elastic properties, chemical composition, etc.) and whose contribution to concrete behaviour also depends on matrix composition and interfacial zone. De Larrard [18] has attributed the role of aggregates on compressive strength to two major characteristics: the aggregate shape and the "maximal paste thickness" between coarse aggregates. According to this author, for rounded aggregates, a decrease in diameter tends to increase the compressive strength. Same kind of results were previously found by Hobbs [28]. Probabilistic model taking into account this effect of aggregates' size distribution on concrete compressive strength was very recently proposed [29] and validated on several experimental data. Experimental indirect tensile tests, performed by Elices and Rocco [30] and compared with many previous experiments, exhibit an analogous trend. Failure in tension remains in a great extent similar to failure in compression (mode I cracking) can be noticed at least at the beginning of the failure process [31]. The complex interactions between this effect of inclusions' size with a pre-cracked and pre-stressed materials, as in the case of a concrete under drying, remains unexplained in details. Even the particular effect of one given diameter for inclusions on mechanical strength is not yet totally known and rather phenomenologically described, particularly on crack nucleation and propagation during mechanical loading. Refined experiments could be of importance to help supporting comprehension of these mechanisms.

It appears that setting up an experimental campaign whose aim is to determine how intimately the strength of a cementitious material is linked to the mesostructure is necessary. However, concretes are very complex materials, with lots of compositions and a great variability, due to the wide range of natural or artificial aggregates that can be used (angulous or rounded shape, granulometric distribution, porosity, roughness, etc.). Trying to analyse the effect of size of inclusions over strength on a real concrete has some advantages, through a better knowledge of the characteristics of this concrete, but due to the numerous factors that should be taken into consideration, the results cannot be extrapolated to other compositions as the physics may remain unknown. As a consequence, it has been decided to conduct these experiments on simplified cementitious materials, based on those proposed by Bisschop and van Mier [1]: composites made of glass beads included in a cementitious matrix. The variation in the mechanical behaviour of such composites for different sizes of inclusion and under drying conditions at different drying states (100–0% water saturation) should therefore be easier to explain by highlighting the physico-chemical phenomena.

For this purpose, in addition to the hydro-mechanical tests in compression on composites described and analysed in the following paragraphs, some complementary data will be proposed through X-ray microtomographic analysis. This technique will allow getting some mesoscale information that will be helpful as evidence for the final drawn conclusions of the effect of dependence of strength with size of inclusions and drying state.

2. Experimental setup

The experimental campaign focuses on underlining the role of aggregates' dimensions on compressive strength, and to what extent the water saturation degree modifies this strength. A detailed description of tested materials, methods of conditioning and drying specimens, experimental devices used to perform uniaxial and triaxial compressive loadings and protocols is given in this section.

2.1. Tested materials

Based on the initial composites proposed by Bisschop and van Mier [1], the composites studied in this campaign are made of a

cementitious matrix surrounding glass beads. These rigid inclusions, essentially made of silica, will act as typical natural siliceous aggregates, even if the shape parameter is not taken into consideration. The choice of spherical non porous smooth inclusions allows minimising the bond strength with surrounding cement paste. This weak ITZ should therefore be more sensitive to drying shrinkage and helps maximising cracks and debonding mechanisms due to aggregate restraining. A worse stress transmission from matrix to inclusions is also expected. Using this type of inclusion should enhance measurable change in strength with drying state and leads to clear conclusions. The main chemical components of those glass inclusions is SiO_2 (65%) and Na_2O (16%). It has to be noticed that alkali-reaction is possible due to this composition (Na_2O can increase the Na^{2+} concentrations of pore fluid, which can product expansive gel in reaction with dissolved SiO_2 in a high pH environment [32]). However this effect is supposed negligible compared to the studied drying effect. The validity of this hypothesis will be supported by some evidence in microtomographic data (§4), where at a sound saturated state, no microcracking can be exhibited.

Four diameters of glass beads are used to create four different composites: C1 with only 1 mm-diameter inclusions, C2 (only 2 mm), C4 (only 4 mm) and C6 (only 6 mm). As the aim of the study is the effect of diameter, the volume fraction of glass inclusions has to remain constant and has been chosen to a value of 35%, the same as initially proposed by Bisschop and van Mier [1]. The second component of this composite is a cement paste, made of CEM I 52.5 N CP2 (according to European standard EN 197-1) with a water-to-cement ratio (W/C) of 0.5. The global composition of the tested composites is summed up in Table 1.

To ensure mechanical tests on sufficient representative samples; it was decided to have at least a minimal sample dimension of 6 times the inclusion diameter. Thus cylindrical samples of 36 mm in diameter and 100 mm in height are cast in stainless steel forms.

As previously mentioned, the interface surface between inclusions can be linked to glass diameter. Table 2 sums up data on this interface and the constitution of the composite. The interfacial surface and the number of particles by mm^3 of material are inversely proportional to inclusion diameter. Hence effects of the weak interface (existence of cracks or debondings due to drying) on compressive strength are expected to be more important in the case of composites C1 rather than for C6. For C1, the number of inclusions is the highest and each one will behave as a rigid point where a crack can nucleate. Inter-distance between cracks should be the lowest and could have an effect on the mechanical strength.

2.2. Sample maturation and drying protocol

All specimens of one type of composite are cast in one time in steel moulds. All composites are cast the same day, to avoid influence of a difference in temperature or humidity when specimens are casted. After 24 h, the samples are demoulded and put in lime-saturated water at 20 °C ± 1 °C for 28 days, to ensure a sufficient maturation, with only slow and few changes of the microstructure due to continuation of hydration process. At the end of this period, the height of sample is reduced to 72 mm (height-to-diameter ratio of 2 for specimens).

Table 1
Constituents of composites.

Composite	C1 to C6
Glass spheres	638.75 kg/m^3
Cement	CEM I 52.5 N CP2 800 kg/m^3
Water	400 kg/m^3
W/C ratio	0.5
Volume proportion of glass spheres	35%

Table 2
Data on inclusions inside composites.

Composite	Inclusion diameter (mm)	Number of inclusion (mm^{-3})	Interfacial surface (mm^2 mm^{-3})
C1	1	0.668	2.10
C2	2	0.084	1.05
C4	4	0.010	0.53
C6	6	0.003	0.35

At this stage, specimens are supposed fully-saturated, and their mass is noted $m_{100\%}$. The dry state (mass $m_{0\%}$) is obtained by putting 6 specimens in an oven at a temperature of 90 °C, which is relatively small to only remove free water contained in the porous network of the cementitious composite. The water content $W_{100\%}$ of a fully-saturated composite is therefore known according to the following equation:

$$W_{100\%} = \frac{m_{100\%} - m_{0\%}}{m_{0\%}} \quad (1)$$

If the hypothesis that the average calculated value of water content is representative for all composites, the water saturation degree S_w of a composite, whose mass is m_i, can be estimated by the following equation

$$S_w = \frac{m_i(1 + W_{100\%}) - m_{100\%}}{m_{100\%}.W_{100\%}} \quad (2)$$

To reach the different water saturation degrees (about 66% and 33%), fully-saturated specimens are placed in an oven at a temperature of 30 °C, which ensures a small temperature gradient and prevents samples from thermal damage. Their weight is regularly measured, until the calculated water saturation degree reaches the desired one. It has to be noticed that due to this protocol, the water saturation is not homogenous through the specimen, because of the low permeability and diffusion properties of such a material. These hydric gradients are one of the causes of cracking inside cementitious materials, and it has to be underlined that cracks due to this "quick" drying (comparatively to a drying through several small steps in relative humidity) are more susceptible to occur in the exterior part of the specimen, whereas the inner part stays sound and with a higher local saturation.

Another point has to be highlighted. After a 28-day maturation, hydration processes still occur, even with low kinetics as formerly stated. However, the time to achieve the different water saturation degrees could modify the maturation level. To solve this issue and to ensure that during the drying time, the maturation will not impact the measured mechanical properties under compression, several specimens at the end of the maturation process (i.e. 28 days after casting) are protected by aluminum foils to prevent water exchange and to stay fully-saturated, and are also placed in the oven at 30 °C. These "witness" samples are tested in uniaxial compression after the same number of days as the 66%, 33% and 0% saturation states are achieved. The peak strength will be compared to the value obtained for fully-saturated specimens tested just after the end of the 28-day maturation, to examine the influence of this additional maturation.

2.3. Mechanical tests

The following paragraphs explain the devices and setups used for the mechanical tests. The surfaces of the specimen where the compressive load is applied are treated to ensure their good

planarity, parallelism and that they are perpendicular to the generatices. All the tests are conducted at 20 °C.

Uniaxial compression tests are performed using a servo-controlled compression tester INSTRON® with a 500-kN capacity. The test is controlled by displacement, with a rate of 0.002 mm/s. Two specimens for each composite and each saturation (100%, 66%, 33% and 0%) are tested. Triaxial tests are performed in a triaxial device developed in the laboratory, composed of a triaxial cell and pumps of a capacity of 60 MPa. The confining pressure is applied by oil pressure. The deviatoric loading is applied by a piston actuated by oil pressure. The oil injection rate is 2 ml/min, until failure of the specimen. In these multiaxial tests, one sample for each composite and each saturation has been used, due to the required time of such experiments.

3. Results and analysis

The results of the previous experiments are presented in this following part. For the sake of simplicity and for a better comprehension, firstly uniaxial strength is dealt with, then triaxial experiments are analysed.

3.1. Uniaxial strength of composites

Fig. 1 sums up the uniaxial compressive strength plotted against the aggregate diameter of composites C1, C2, C4 and C6 (which are respectively 1, 2, 4 and 6 mm) for four different water saturation degrees, ranging from a fully saturated specimen (noted as 100%) to a dry one (0%, which means for a dry state at 90 °C), with two intermediate states (about 66% and 33%). Each dot is the average value of two tests.

If the fully-saturated specimens are observed, it can be clearly noticed that a great correlation between glass diameter and strength exists. Indeed, whereas for composites C6 the uniaxial strength is 19.4 MPa, this value increases with lower diameters, very slightly for C4 (only 4% higher than for C6) but intensively for C2 (63% higher) and C1 (118% higher). For these saturated samples kept under lime-saturated water until the day of compressive test, the initial microstructure of the cementitious matrix is about the same as the same maturation process has been performed. The only reason why this initial microstructure might have been modified is a differential effect of dimensional variations of the matrix during maturation process due to the presence of different diameters for the composites. However, as the samples were stored in water and have a W/C ratio of 0.5, the self-desiccation is expected to be low (external water can enter the specimen to compensate the water consumption during hydration, preventing shrinkage).

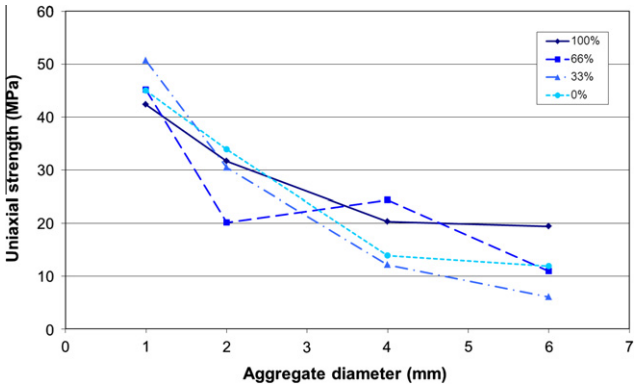

Fig. 1. Uniaxial compressive strength versus aggregate diameter. Four water saturation degrees are tested (100%, 66%, 33% and 0%).

Hence, any observation made onto these composites can rely on this hypothesis of the same initial state of the matrix.

The change in measured strength must therefore be attributed to the change in inclusion diameter and its effects on failure of the specimens, and as previously explained, the potential effect of a greater proportion in interfacial zones for composites with lower diameters, linked to a higher specific surface for these composites. As a result, the increase in strength with lower diameter can probably be attributed to a change in the stress repartition inside the specimen. Each aggregate, which acts as a rather rigid inclusion inside a deformable matrix, will tend to restrain the contraction of the matrix under compressive load, comparatively to a specimen without rigid inclusions. Consequently, it will lead to a development of a locally non homogenous state of stresses around each inclusion, which depends on the aggregate diameter as explained in the introduction. During the compressive loading, stresses around inclusions evolve until they locate in one specific area, they reach the strength of the matrix, leading to plasticity and/or damage and crack. However, when inclusions are smaller and their number is therefore higher, the quantity of locations where cracks can nucleate is higher and the local stress concentrations due to inclusions are expected to be lower and globally more widespread through the whole specimen (i.e. around a greater number of inclusions). This explanation seems to match the measured evolution of uniaxial strength with diameter of Fig. 1 for fully saturated composites. As a consequence, this effect appears to be predominant compared to the interfacial area effect. Indeed, when smaller inclusions are used, the interfacial zones, with reduced mechanical properties, are in proportion more numerous. A decrease in strength would have been expected as diameter is reduced if it was the predominant mechanism. However, that was not the case at least for fully saturated specimens. One reason can explain this observation. The thickness of this interfacial zone may be very small for an interface between the matrix and a non porous aggregate (glass beads were used here), and the results cannot put in evidence that this area plays a significant role on the strength.

To try to validate and complete the previous explanations, the evolution of strength with diameter for partially or totally dried composites in Fig. 1 is analysed. It appears that the same tendency can be noticed with a better strength as the diameter of inclusion is reduced, whatever the water content. Nevertheless, if the curves are more deeply studied, some additional effects can be observed, due to the applied drying before the compressive test.

Firstly, for the composite C6, the partial drying at a water saturation of 66% or 33% tends to weaken the uniaxial strength in a great extent, with a decrease from 19,4 MPa at a saturated state to 10.9 MPa at 66% (decrease of 44%) and even 6 MPa at 33% of saturation (decrease of 69%). This phenomenon can be attributed to the desiccation shrinkage, which involves in an heterogeneous cementitious material two competitive effects. The capillary and disjoining pressures [33,34], which auto-stress the material and act as "external" confinement, play a role that leads to a reinforcement of the strength [35]. On the contrary, the differential shrinkage between matrix and rigid inclusions and also between outer and inner zone of the specimen lead to cracking. This negative effect appears as predominant in comparison with an increase in auto-confining by capillary and disjoining pressures. For the fully-dried composites C6, the uniaxial strength is 11.9 MPa which could indicate that lowering the water saturation after 33% mainly has an effect on the auto-confining effect rather than cracking. The same conclusion can be drawn for C4 except for a saturation of 66% which is higher than for the fully saturated sample.

Secondly, if the results for C2 and C1 are being investigated, the great drop in uniaxial strength between 100% and 33% saturated composites does not exist anymore. For instance for C2, only a small decrease of 4% is measured, and even a small increase of

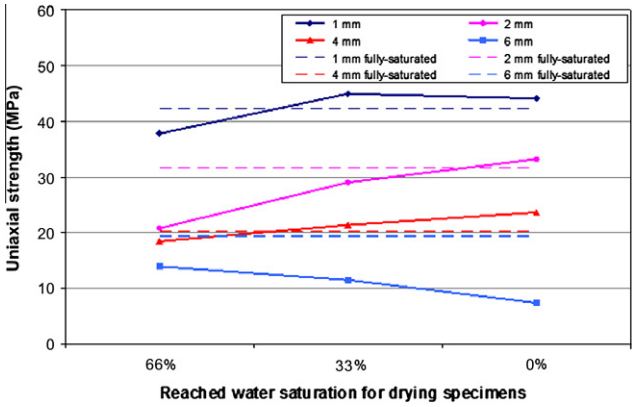

Fig. 2. Uniaxial strength of witness samples (protected from desiccation) of C1 (1 mm), C2 (2 mm), C4 (4 mm) and C6 (6 mm) tested the same day than composites under drying with a saturation of about 66%, about 33% or 0%. The dashed lines stands for the uniaxial strength measured on fully-saturated composites.

7% between 100% and 0% saturation. For C1, even a uniaxial strength increase of 20% (between 100% and 33% saturation) is noted. Although the cementitious matrix is the same as for C4 and C6 and in the same volume fraction, such results indicate a change in the predominant effect linked to drying shrinkage. For the composites with smaller aggregates, the auto-confining effect overlaps the cracking one, which implies a change in the mechanical behaviour of the composites. Thus, if the cracking effect is reduced without other changes in the microstructure of the matrix, this underlines an important modification in the cracking pattern relying on the diameter of aggregates, as yet supposed when dealing with fully-saturated composites.

To validate that maturation will not imply too many changes when comparing the evolution of strength with drying, strength of witness samples is checked. The witness samples are kept under endogenous conditions after 28 days of curing in lime saturated water and tested in uniaxial compression the same day as those which were in drying conditions to reach their wanted saturation. Fig. 2 presents the measured uniaxial strength of the witness samples, and is compared to the uniaxial strength of fully-saturated composites (dashed lines). For composites C1 and C4, the strength values of witness samples and the fully saturated ones match, although a small increase in strength is observed for performed tests at the same day as 33% and 0% saturated samples. It should be noticed that the aluminium protection to ensure the endogenous conditions is not totally perfect, as saturations of witness samples vary between 88% and 98%. Some slow drying shrinkage can therefore be possible, even if it remains limited and could partly explain this small increase. The maturation effect is therefore small. For C2 composites, the increase in respect with time of test is more pronounced than for C1 and C4, and the first value (day of test of 66% saturated composites) which could be expected to be closer from fully-saturated state is actually the furthest. One of the two strengths measured on these samples is quite low (18.3 MPa) and perhaps should be discarded due to experimental problems. For C6 composites, the trend goes the other way round, with a decrease in strength. The small loss of water due to imperfect aluminum foil protection could lead to cracking (since strength of C6 seems to be the most influenced by drying) and a drop in strength. In this case, it is difficult to distinct the effect of this drying and the maturation effect, even if it appears that for C1, C2 and C4, additional hydration is low.

As a partial conclusion, uniaxial tests highlight two main phenomena. The first one is the great dependency of uniaxial compressive strength to inclusion diameter, independently from water saturation: the larger the aggregate, the lower the uniaxial strength. The second one is a change in the effect of the drying shrinkage according to the diameter of aggregates: whereas for larger inclusions a previous partial or total drying greatly reduced the strength of the composites, for the smallest inclusions it tends to have no effect or even to enhance this strength. This is supposedly attributed to a differential cracking pattern between C1, C2, C4 and C6 composites. A turning point between predominance of each competitive effect appears to be around an inclusion diameter of 2 and 4 mm. One first possible way to investigate this change in cracks is to allow them to play a higher mechanical role, or not, for example during multiaxial compression -i.e. opening or closing the cracks and verifying the effect on the compressive strength.

3.2. Multiaxial strength

Triaxial compression tests are therefore performed by applying a confining pressure to the composite which will allow to study the mechanical behaviour of composites in multiaxial states of stress and also to get data on the influence of cracks. Indeed the confinement tends to close every cracks and micro-cracks provided that its value is high enough. Hence the studied confining pressures are 5 and 15 MPa, which are two levels with a different state of closure of cracks.

Fig. 3 presents the deviatoric strength of composites versus the diameter of aggregates for a confining pressure of 5 MPa, which ensures a partial closure of cracks. The deviatoric strength is defined as the difference between the axial stress (in the direction where the compressive load is applied) and the confining pressure. Each point is the measure on only one specimen, due to the time needed to perform such a triaxial test. In addition, a weak defect inside the composite (crack, void, etc.) could be the cause of the initiation of the whole sample failure under uniaxial compression. But the confining pressure in multiaxial compression might decrease the effect of this weakest link on the strength. Expected variability is therefore lower in triaxial tests, but the results remain more qualitative.

As in the previous part, tests are performed under the same water saturation conditions: fully or partially saturated specimens (100%, 66% or 33%) and specimens at a dry state. For such a confining pressure, the fully saturated composites exhibit, as expected, a higher deviatoric strength than in the uniaxial compressive tests for all aggregate diameters. Moreover, as for uniaxial compression, an increase of deviatoric strength is noticed with a decreasing diameter of inclusions. More precisely, only a slight increase is observed by reducing the diameter from 6 to 4 mm and even 2 mm, but a more pronounced one appears when the diameter is reduced to 1 mm (increase of 42% compared to C6). This observation is in accordance with the one made in uniaxial compression, thus indicating a clear effect of the diameter of inclusions over the

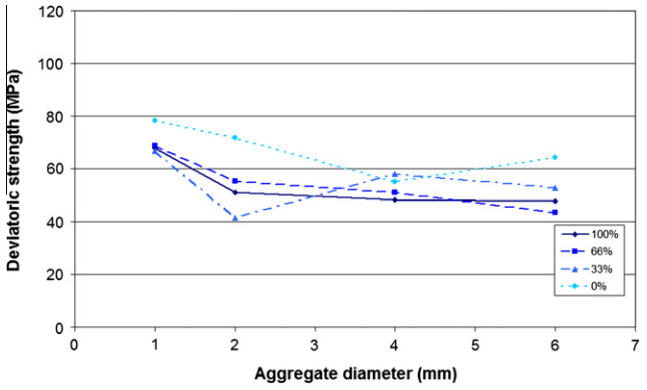

Fig. 3. Deviatoric strength versus aggregate diameter for confining pressure of 5 MPa. Four water saturations are tested (100%, 66%, 33% and 0%).

mechanical behaviour, even in a triaxial state of stresses, reinforcing the previous conclusions.

The effect of the confinement can also be studied on partially saturated or dried specimens. The notable thing to analyze is that for C6 composites, the drastic drop in strength observed by partially drying the specimens cannot be seen anymore. The 66% saturated composite only shows a 9%-decrease in strength compared to the fully saturated sample. In addition, in deeper steps of drying, there is even an increase in strength (11% for 33% saturated specimens, 35% for the dried one). This behaviour is attributed to the partial closure of cracks due to the drying effect under such a confinement. Therefore, if the negative effect of cracking over strength is limited by the confining pressure (partial closure of cracks), mainly the positive effect of capillary and disjoining pressures play a role. This seems to be validated also on C4 and C2 composites, even if the value of the 33% saturated C2 appears to be quite low compared to the expected value. This is probably due to the inherent variability of the specimen. For the C1 composites, the increase in strength with desiccation remains quite lower compared to C2 but mainly C4 and C6. This should be explained by the argument proposed in the previous part. Indeed, the cracking pattern is supposedly playing a less important role for the lowest diameters, and the increase in strength observed in Fig. 1 was attributed mainly to the benefic effect of capillary and disjoining pressures. In Fig. 3 for C1, there is as a consequence fewer cracks, or at least, a different cracking pattern that the confining pressure will not close as clearly, mechanically speaking, as for C6 composites. The fact that the cracking pattern will be quite different according to diameter inclusions and not influence in the same way the mechanical strength of a composite seems to show evidence of its validity.

Fig. 4 presents the same results on composites as for Fig. 3, but with a confining pressure of 15 MPa which will close more cracks and should reinforce the conclusions drawn from Fig. 3. Indeed, the analysis of the curves again highlights the same phenomenon. An increase of the deviatoric strength with a reduced diameter of inclusions is noticed for fully saturated specimens. The jump in strength for dried C6 is even higher than previously, and this effect could rely on the drying conditions for reaching such a state (oven dried specimen at 90 °C) which could lead to more damage and cracks of the cementitious matrix. Only one main change seems to occur for C2 composites, where the evolution of strength with drying is quite small, particularly for the dried state where a small decrease in strength happens, but this can be due to an experimental uncertainty. Finally, if the evolution of the strength for dried composites is studied, one could remark that the strength is about at the same level for C1 and C6, whereas it is noticeably lower for C2 and C4. However it has previously been observed that for all specimens at given water saturation, reducing the inclusion diameter increases the strength. This could be probably explained by the differential cracking pattern among those composites and perhaps a role of the interfacial transition zone whose volume proportion in C6 is lower than in C1. Thus, as this interface is known to have a reduced mechanical strength, a more important proportion should decrease the global strength of C1, even if this effect cannot be clearly detected under lower confining pressure.

Hence the influence of the diameter of aggregates over strength seems to be well underlined for triaxial compression. Another evidence of an existence of different cracking patterns for each kind of composites, which will differently modify the mechanical behaviour of the material, is also put in light.

3.3. Failure surface

The main physical mechanisms and parameters to take into consideration have to be highlighted, which was the issue of the former parts. From the obtained results, it is also possible to draw the failure surface of the tested composites, as several loading paths have been tested (uniaxial compression and triaxial compression under two different confining pressures). Theses curves can be helpful when aiming at modelling the behaviour of cementitious composites, by the knowledge on which parameter will modify the failure surface (drying state, diameter of inclusions). The failure surfaces are drawn in the (p, q)-plan where p and q are defined as follows:

$$\begin{aligned} p &= \tfrac{1}{3} tr(\overline{\overline{\sigma}}) \\ q &= \sqrt{\tfrac{3}{2}\overline{\overline{s}} : \overline{\overline{s}}} \end{aligned} \tag{3}$$

where $\overline{\overline{\sigma}}$ is the Cauchy stress and $\overline{\overline{s}}$ the deviatoric part of the Cauchy stress.

3.3.1. Effect of aggregate diameter

Fig. 5a and b presents the failure surfaces for C1 (1 mm) to C6 (6 mm) composites for the two extreme water saturation conditions, that is to say fully-saturated (Fig. 5a) and totally dried (Fig. 5b) specimens to underline better the effect of the diameter of inclusions.

On Fig. 5a, at a saturated state, the shape of the failure surface is identical for the four composites, with a more important first slope when mean pressure p remains low (until a confining pressure of 5 MPa) than the second one as confinement increases. However, reducing the diameter of aggregates will mainly decal towards higher q value, mainly for C1 composite which is consistent with the conclusions drawn in §3.2. Therefore if the failure surface has

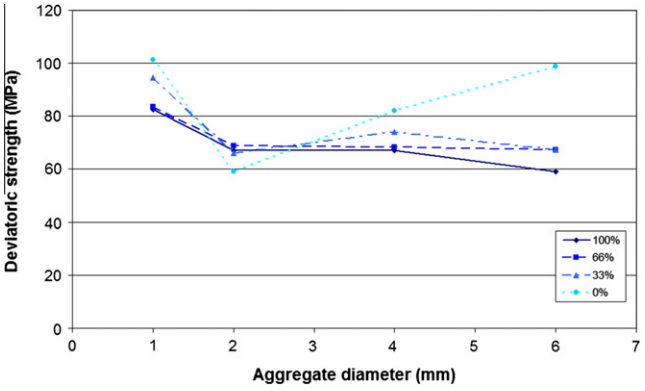

Fig. 4. Deviatoric strength versus aggregate diameter for confining pressure of 15 MPa. Four water saturations are tested (100%, 66%, 33% and 0%).

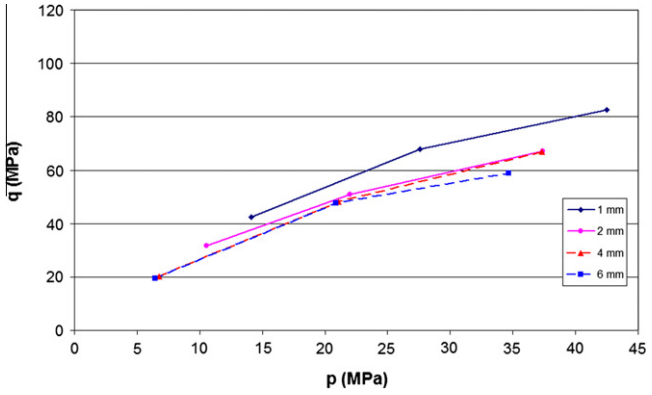

Fig. 5a. Failure surface of the composites C1 (diameter of inclusions: 1 mm), C2 (2 mm), C4 (4 mm) and C6 (6 mm) in the fully-saturated state (100%).

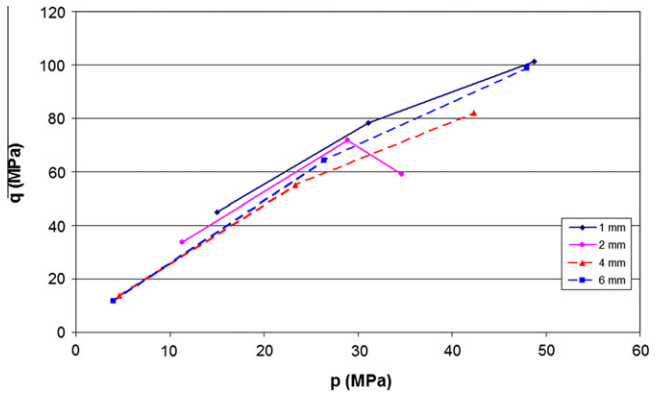

Fig. 5b. Failure surface of the composites C1 (diameter of inclusions: 1 mm), C2 (2 mm), C4 (4 mm) and C6 (6 mm) in the fully-dried state (0%).

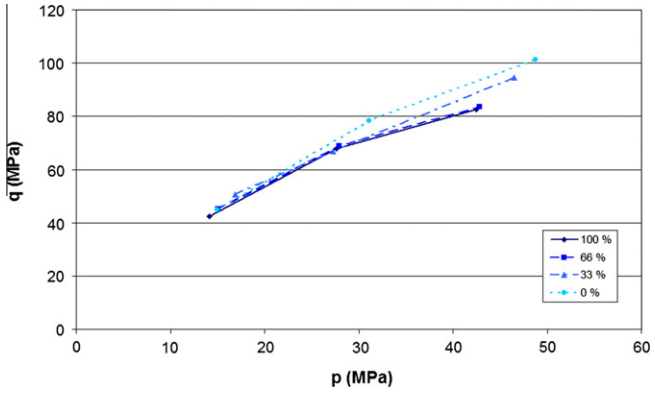

Fig. 6a. Failure surface of the composite C1 under different water saturations (100%, 66%, 33% and 0%).

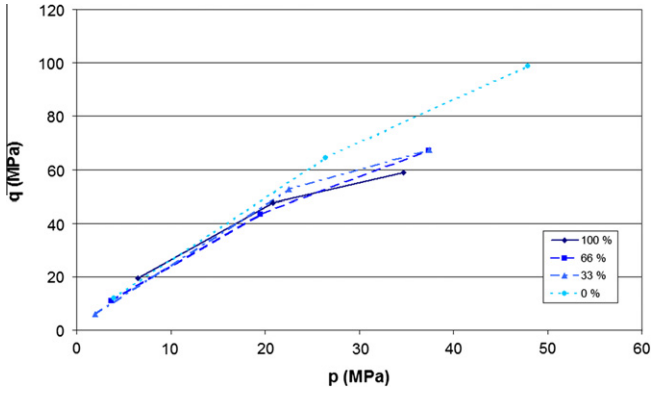

Fig. 6b. Failure surface of the composite C6 under different water saturations (100%, 66%, 33% and 0%).

to be modelled in a numerical approach, the diameter of inclusions has to be included as a parameter.

The same observations are made on Fig. 5b, even if the decal towards higher values of q with reducing diameter of inclusions is less pronounced. That could be linked to the existence of a cracking pattern and interstitial pressures due to the drying of the specimens. The experimental erroneous value for C2 composite under high confining pressure is again shown, and must lead to discard this value.

3.3.2. Effect of water saturation degree

On the other hand, it could be of interest to draw the failure surface for one given composites under a varying water saturation from 100% to 0%. Fig. 6a and b shows these results for C1 (Fig. 6a) and C6 (Fig. 6b) composites.

The shape of the failure surface is, as expected, the same as in §3.3.1, with a decreasing slope when the value of p is increased. The influence of the drying state is well shown. Thus, for low values of p, the surface remains the same for each saturation. This is noticed for both C1 and C6 composites. In the second part of the surface, the behaviour starts being different, with a less important decrease of the slope as far as saturation decreases, due to the capillary pressure and disjoining pressure that tend to increase the peak strength by additional auto-confining effect. The effect of drying is therefore mainly to be taken into consideration for high values of confinement (high values of p).

4. Microtomographic evidence

The advanced hypothesis that the cracking pattern is different for each composite is based on the observed change in mechanical behaviour in multiaxial compression. An additional experimental evidence is proposed to confirm it, by means of imagery technique of the cracking pattern of composites: X-ray microtomography, which allows non-destructive imagery of a sample at different states of degradation [36]. The global principle relies on differential X-ray attenuation by the different constituents of the composite. A set of 2D radiographs of the specimen is taken under various angles, and through a filtered backprojection algorithm, a 3D map of attenuation coefficient is obtained with a resolution of 5.3 μm. As glass beads, cementitious matrix and void have different attenuation coefficients, it is possible to read the 3D map as a 3D image of the specimen. A deeper description of principles X-ray microtomography can be found in [37] and the detailed setup of the microtomographic acquisition in [38].

This experimental campaign is performed on similar cement-glass beads composites as those tested in uniaxial and triaxial compression (Table 1), but the cement used is a CEM II/B 32.5 R LL-S, that is to say with mainly Portland cement, and a small part of blast-furnace slag and calcareous additions. However, even if the cementitious matrix will have a slight different constitution, and some different values in mechanical behaviour or in desiccation shrinkage, the obtained results will be useful as the only expected goal is to show a change in the cracking pattern for a shrinking cementitious matrix with glass rigid inclusions. The composites based on this modified formulation are named D1 to D4 (for inclusions of 1 to 4 mm in diameter).

Prismatic beams (40∗40∗160 mm) of D1, D2 and D4 are cast, then demoulded after 24 h and kept in lime-saturated water at 20 °C for 28 days. Then, they are covered with aluminum sheets to keep them in endogenous conditions. Small cylindrical specimens (diameter: 8 mm – height: about 20 mm) are cored from these beams and a microtomographic acquisition is performed at this step. Finally, these specimens are kept in an oven at a temperature of 60 °C for 24 h before performing a new microtomographic acquisition, and being able to observe changes in the microstructure, and mainly apparition of cracks. The choice of such an accelerated drying test was due to the allowed time at ESRF (European Synchrotron Radiation Facility, Grenoble, France) where microtomography was performed.

For the presentation of results, 3D maps are not included since complex to analyse and comment. 2D numerical slices extracted from the reconstructed three-dimensional images are shown. Fig. 7 shows 2D slices from composites D1 (Fig. 7a), D2 (Fig. 7b) and D4 (Fig. 7c) before drying. The constituents are clearly visible

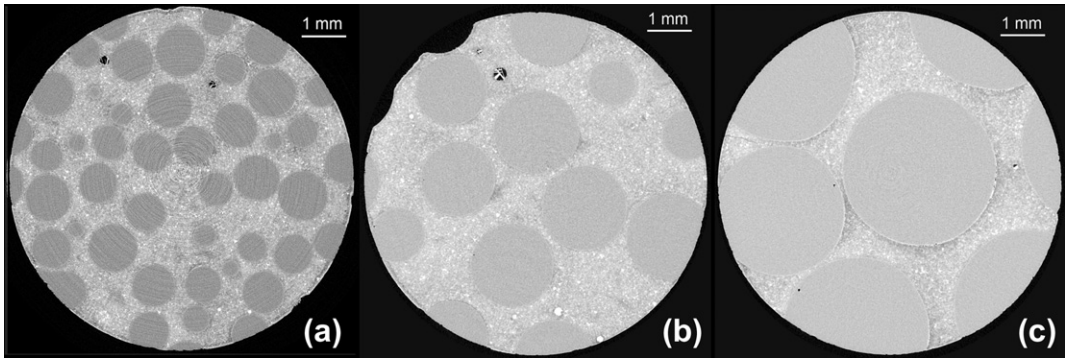

Fig. 7. 2D mictrotomographic slices of composites D1 (a), D2 (b) and D4 (c) before drying (sound state). Images (b) and (c) have been filtered.

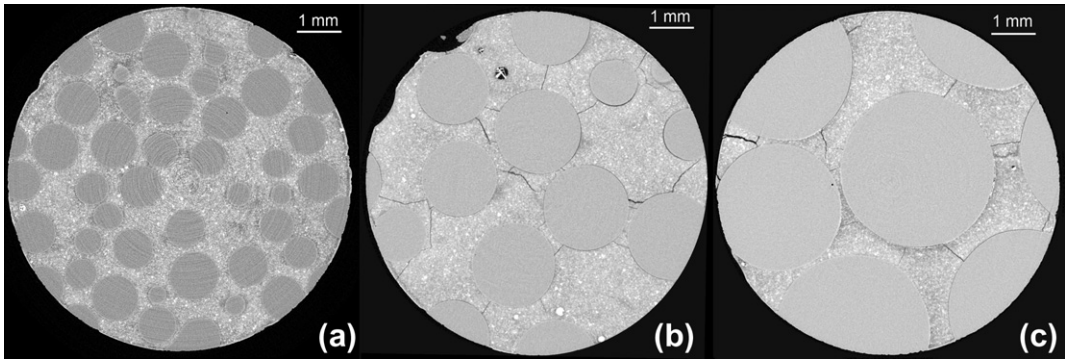

Fig. 8. 2D mictrotomographic slices of composites D1 (a), D2 (b) and D4 (c) after 24 h of drying at 60 °C (dried state). The slice of composite D1 is not at the same location than at the sound state. Images (b) and (c) have been filtered.

(glass inclusions, cementitious matrix) and also trapped air bubbles which appear as dark. Whatever the composite in this sound state, no cracks are visible, indicating that the cementitious microstructure, at a resolution of 5.3 μm, is similar for all composites.

Slices of the same specimens are presented in Fig. 8, but after the drying of the specimen at 60 °C. On Fig. 8a (composite D1), the microstructure appears to be unchanged compared to Fig. 7a. Indeed, no cracks are clearly visible after such a drying, indicating that if the microstructure has changed, the resolution of the performed microtomography is not sufficient to detect it. By studying Fig. 8b (composite D2), a great modification exists as a crack network can be detected. The cracks are localised essentially between the surface of the specimen and an inclusion, between two inclusions and finally around inclusions (debonding cracks). These cracks are due to drying shrinkage of the cementitious matrix, and will mainly occur near rigid inclusions, which prevent free shrinkage and the existence of localised heterogeneous stresses. The presence of cracks at the interface matrix-inclusion tends to indicate that indeed an interfacial zone with weak mechanical properties exists, but cannot give additional data on its role over the global response of the composite under compressive loads. From these observations, it is highlighted that the cracking pattern is strongly dependant to the diameter of inclusions. This is reinforced by the cracks on the D4 composites (Fig. 8c), which are at the same locations as for D2. However, due to a lower number of inclusions by cubic millimetre of composite (Table 2), the number of cracks is reduced, and the mean length and opening is likely to be modified. Such a change in the cracking network will therefore influence the global mechanical behaviour of the composite under compressive loadings for example, but this could also have an influence on other physico-chemical properties linked to durability (permeability, diffusivity, etc.). These results are in accordance with Grassl et al. [39], who found an increase of the average crack width and permeability with increasing aggregates diameter. This microtomographic analysis has brought evidence that the diameter of inclusions is strongly linked to the mechanical behaviour of the partially and totally dried specimen, and enhanced the conclusions on water saturation effects drawn in the §3. Here, the cracks studied are due to a drying of the samples, resulting from shrinkage of the matrix. Some evidence of this role over cracking repartition was initially observed by Bisschop and van Mier [1]. Analogous conclusions could be expected for cracks generated by compressive loadings, explaining that the nucleation and propagation of cracks is hardly linked to inclusion diameter, potentially being at the origin of the evolution of strength measured for fully saturated specimens. The exact quantification of the cracking pattern still needs some developments in image analysis. Moreover the quantification of cracks might be unreliable as a variable part between composites would be hidden (due to the resolution of the microtomographic acquisition (5.3 μm) and the crack width dependent on inclusion diameter). This quantification (orientation, width, length...) and its use as parameter in numerical modelling could help justifying the fact that many small cracks seems to lead to higher strength than few small cracks.

Finally, a possible coupling effect between the existence of drying cracks and change in capillary effect linked to compressive strength has not been considered in this study. The coupling is assumed to be low as only very small cracks (smaller width than pores still water saturated in partially saturated conditions) would be involved in a change of the confining capillary pressure effect

over strength. Some further investigations should be done to definitively validate this assumption.

5. Conclusion

The experimental campaign performed on geometrically simplified cementitious composites cement-glass beads underlined a noticeable effect of the size of inclusions over the uniaxial and triaxial compressive strengths. Hence for saturated materials, an increase of this strength with a reducing diameter of inclusions has been experimentally observed and does not follow a linear relation. Indeed, the significant jump in strength is for the smallest aggregates (C1 composite), whereas for C2 and C4 the increase is less important. Physical descriptions of compressive behaviour in numerical models should therefore take this diameter of aggregates into consideration, and not only be focused on volume fraction of inclusions.

In addition, if coupled hydro-mechanical behaviour is studied, the dependence of the cracking pattern due to drying has been highlighted. The water saturation, as expected, tends to have two main competitive effects: an increase in strength due to auto-confining by capillary and disjoining pressures when water saturation is decreased and a reduction of strength due to cracking involved by drying shrinkage. From the uniaxial and triaxial results performed on C1 to C6 composites (with an apparent turning point between aggregate diameter of 2 and 4 mm), it shows that the cracking pattern is quite different between all composites, providing the changes in strength measured under low or high confining pressure which allows to modify the importance of the effect of cracks over the global mechanical response of the samples. A possible small influence of the interfacial zone between cementitious matrix and aggregates has also been supposed.

Additional X-ray microtomographic experiments have been conducted to validate with 3D imaging at high resolution (about 5 μm) the conclusions drawn from analysis of the compressive behaviour of composites. It appears that, indeed, the cracking pattern induced by drying is highly dependent to diameter of inclusions: the opening of cracks, if they exist, remains below 5 μm for inclusions of 1 mm, whereas for 2 or 4 mm, it can reach as high as 20 μm. Moreover, the number of cracks is influenced by the number of inclusions in a volume of composites. These changes in the morphology of the cracking pattern could be at the origin of disparate behaviour between the different composites under drying, but also could partially explain the change in compressive strength on saturated samples, which implies a propagation of cracks to reach that peak strength. The existence of the interfacial zone has also been noticed since numerous cracks are detected at this location, which is an evidence of mechanical reduced properties, even if this zone is submitted to highly heterogeneous stresses.

Future works are being performed mainly in the framework of the ANR Microfiss project notably to enhance the comprehension of the behaviour of those kinds of composites under compression. The key idea is to validate how cracks nucleate and propagate, and particularly how this is modified by the presence of rigid inclusions inside a cementitious matrix. For example, such results will allow to confirm the given conclusions in this paper on the rack pattern dependency to inclusion diameter.

Acknowledgments

Authors thank ESRF (European Synchrotron Radiation Facility) of Grenoble (France) for the access to the synchrotron facility in beamline BM05 and also ANR Microfiss for financial support.

References

[1] Bisschop J, van Mier JGM. Effect of aggregates on drying shrinkage microcracking in cement-based composites. Mater Struct 2002;35(8):453–61.
[2] Ollivier JP, Vichot A. Durabilité des bétons. 2nd ed. Presses de l'école nationale des Ponts et Chaussées (ENPC); 2008 [in French].
[3] Pijaudier-Cabot G, Gérard B, Acker P Creep. Shrinkage and durability of concrete and concrete structures. London: Hermes Science Pub.; 2005.
[4] Burlion N, Bourgeois F, Shao JF. Effects of desiccation on mechanical behaviour of concrete. Cem Concr Compos 2005;27(3):367–79.
[5] Pihlajavaara SE. A review of some of the main results of a research on the ageing phenomena of concrete: effect of moisture conditions on strength, shrinkage and creep of mature concrete. Cem Concr Res 1974;4(5):761–71.
[6] Yurtdas I, Burlion N, Skoczylas F. Triaxial mechanical behaviour of mortar: effects of drying. Cem Concr Res 2004;34(7):1131–43.
[7] Popovics S. Effect of curing method and moisture condition on compressive strength of concrete. ACI J. 1986;83(4):650–7.
[8] Bangert F, Grasberger S, Kuhl D, Meschke G. Environmentally induced deterioration of concrete: physical motivation and numerical modelling. Eng Fract Mech 2003;70(7–8):891–910.
[9] Bary B, Bournazel JP, Bourdarot E. Poro-damage approach applied to hydro-fracture analysis of concrete. J Eng Mech 2000;126(9):937–43.
[10] Bisschop J, van Mier JGM. How to study drying shrinkage microcracking in cement-based materials using optical and scanning electron microscopy? Cem Concr Res 2002;32(2):279–87.
[11] De Sa C, Benboudjema F, Thiery M, Sicard J. Analysis of microcracking induced by differential drying shrinkage. Cem Concr Compos 2008;30(10):947–56.
[12] Hearn N. Effect of shrinkage and load-induced cracking on water permeability of concrete. ACI Mater J 1999;96(2):234–41.
[13] Lagier F, Jourdain X, De Sa C, Benboudjema F, Colliat JB. Numerical strategies for prediction of drying cracks in heterogenous materials: Comparison upon experimental results. Eng Struct 2011;33(3):920–31.
[14] Pindera MJ, Khatam H, Drago AS, Bansal Y. Micromechanics of spatially uniform heterogeneous media: a critical review and emerging approaches. Composites: Part B 2009;40(5):349–78.
[15] Maghous S, Dormieux L, Barthelemy JF. Micromechanical approach to the strength properties of frictional geomaterials. Eur J Mech – A/Solids 2009;28(1):179–88.
[16] Dormieux L, Kondo D, Ulm FJ. Microporomechanics. Wiley; 2006.
[17] Bentz DP. A review of early-age properties of cement-based materials. Cem Concr Res 2008; 38(2). The 12th international congress on the chemistry of cement. Montreal, Canada; July 8–13 2007. p. 196–204.
[18] De Larrard F. Concrete mixture-proportioning – a scientific approach. Modern concrete technology series, No. 9, E & FN SPON, London; 1999.
[19] Diamond S, Huang J. The ITZ in concrete – a different view based on image analysis and SEM observations. Cem Concr Compos 2001;23(2–3):179–88.
[20] Ollivier JP, Maso JC, Bourdette B. Interfacial transition zone in concrete. Adv Cem Based Mater 1995;2(1):30–8.
[21] Hashin Z, Monteiro PJM. An inverse method to determine the elastic properties of the interphase between the aggregate and the cement paste. Cem Concr Res 2002;32(8):1291–300.
[22] Rangaraju PR, Olek J, Diamond S. An investigation into the influence of inter-aggregate spacing and the extent of the ITZ on properties of Portland cement concretes. Cem Concr Res 2010;40(11):1601–8.
[23] Zheng J, Wong HS, Buenfeld NR. Assessing the influence of ITZ on the steady-state chloride diffusivity of concrete using a numerical model. Cem Concr Res 2009;39(9):805–13.
[24] Carde C, François R. Effect of ITZ leaching on durability of cement-based materials. Cem Concr Res 1997;27(7):971–8.
[25] Bisschop J, Pel L, van Mier JGM. Effect of aggregate size and paste volume on drying shrinkage in cement-based composites. In: Ulm FJ, Bazant ZP, Witmann FH, editors. Creep, shrinkage and durability mechanics of concrete and other quasi-brittle materials. Proceedings of the 6th international conference concreep ; 2001.
[26] Cauvin L, Kondo D, Brieu M, Bhatnagar N. Mechanical properties of polypropylene layered silicate nanocomposites: characterization and micro-macro modelling. Polym Test 2010;29(2):245–50.
[27] Cho J, Joshi MS, Sun CT. Effect of inclusion size on mechanical properties of polymeric composites with micro and nano particles. Compos Sci Technol 2006;66(13):1941–52.
[28] Hobbs DW. The compressive strength of concrete: a statistical approach to failure. Magaz Concr Res Stat 1972;24(80):127–38.
[29] Miled K, Limam O, Sab K. A probabilistic mechanical model for prediction of aggregates' size distribution effect on concrete compressive strength. Phys A: Stat Mech its Appl 2012;391(12):3366–78.
[30] Elices M, Rocco CG. Effect of aggregate size on fracture and mechanical properties of a simple concrete. Eng Fract Mech 2008;75(13):3839–51.
[31] Carpinteri A, Chiaia B, Nemati KM. Complex fracture energy dissipation in concrete under different loading conditions. Mech Mater 1997;26:93–108.
[32] Fournier B, Bérubé MA. Alkali-aggregate reaction in concrete: a review of basic concepts and engineering implications. Can J Civil Eng 2000;27:167–91.
[33] Baroghel-Bouny V, Godin J. Experimental study on drying shrinkage of ordinary and high-performance cementitious materials. In: Baroghel-Bouny V, Aitcin PC, editors. Shrinkage of concrete. Paris: RILEM, Publication; 2000. p. 215–32.

[34] Yurtdas I, Burlion N, Skoczylas F. Experimental characterisation of the drying effect on uniaxial mechanical behaviour of mortar. Mater Struct 2004;37(3):170–6.
[35] Wittmann FH. Creep and shrinkage mechanisms. In: Bažant ZP, Wittmann FH, editors. Creep and shrinkage in concrete structures. Chichester: Wiley; 1982. p. 129–61.
[36] Bernard D, Vignolles GL, Heintz JM. Synchrotron X-ray micro-tomography: a tool for porous materials evolution modelling. In: Baruchel J, Buffière JY, Maire E, Merle P, Peix G, editors. X-ray tomography in materials science. Paris: Hermès, Science; 1999. p. 177–92.
[37] Landis EN, Keane DT. X-ray microtomography. Mater Charact 2010;61(12):1305–16.
[38] Rougelot T, Burlion N, Bernard D, Skoczylas F. About microcracking due to leaching in cementitious composites: X-ray microtomography description and numerical approach. Cem Concr Res 2010;40(2):271–83.
[39] Grassl P, Wong HS, Buenfeld NR. Influence of aggregate size and volume fraction on shrinkage induced micro-cracking of concrete and mortar. Cem Concr Res 2010;40(1):85–93.